Applied Catalysis A: General 517 (2016) 73–80

Contents lists available at ScienceDirect

Applied Catalysis A: General

journal homepage: www.elsevier.com/locate/apcata

Dehydration of 5-amino-1-pentanol over rare earth oxides

Kaishu Ohta, Yasuhiro Yamada, Satoshi Sato *

Graduate School of Engineering, Chiba University, 1-33 Yayoi, Inage, Chiba 263-8522, Japan

ARTICLE INFO

Article history:
Received 16 December 2015
Received in revised form 2 February 2016
Accepted 1 March 2016
Available online 3 March 2016

Keywords:
Catalytic dehydration
Amino alcohol
Unsaturated amine
Rare earth metal oxides

ABSTRACT

Vapor-phase catalytic dehydration of 5-amino-1-pentanol was investigated over various oxide catalysts including rare earth oxides (REOs). Over ordinary acidic oxides such as Al_2O_3, SiO_2, SiO_2-Al_2O_3, TiO_2, and ZrO_2, a cyclic amine such as piperidine was mainly produced at temperatures of 300 °C and higher. In contrast, basic REOs with a cubic bixbyite structure showed the catalytic activity in the conversion of 5-amino-1-pentanol to produce 4-penten-1-amine at 425 °C. In REO catalysts, Tm_2O_3, Yb_2O_3, and Lu_2O_3 showed the high conversion of 5-amino-1-pentanol and the high selectivity to 4-penten-1-amine. Especially, Yb_2O_3 calcined at 800 °C showed a high formation rate of 4-penten-1-amine with the selectivity of ca. 90% at 425 °C. In comparing the reactivity of several amino alcohols to form the corresponding unsaturated amines, Yb_2O_3 effectively catalyzed the dehydration of 6-amino-1-hexanol into 5-hexen-1-amine, whereas 3-amino-1-propanol and 4-amino-1-butanol were not effectively dehydrated due to the decomposition of the reactant.

1. Introduction

Unsaturated amines, which have both a carbon double bond and an amino group in the molecule, can be used for various applications such as polymer, ion-exchange membrane, raw material of chemical, pharmaceutical and agricultural chemical intermediates. As a pioneering report, Zimmermann et al. have reported that unsaturated amines can be produced by hydroaminomethylation of olefins using three gases such as H_2, CO, and NH_3 [1]. In the method, however, the resulting primary amines are further converted into the secondary amine. Nicolai et al. have showed that 4-penten-1-amine is produced by reduction of 4-pentenamido [2], while 4-penten-1-amine is produced with a low yield, which is approximately 40%.

We have previously reported a novel catalytic synthesis process of unsaturated alcohols via the dehydration of alkanediols such as 1,5-pentanediol [3–5], 1,4-butanediol [5–8], and 1,3-butanediol [5,9–11] over rare earth oxides (REOs) calcined at 800 °C. In the dehydration of 1,5-pentanediol, heavy REOs such as Lu_2O_3, Yb_2O_3, and Tm_2O_3 are highly active and selective for the formation of 4-penten-1-ol, and the highest selectivity of 4-penten-1-ol was 80.3% over Tm_2O_3 calcined at 800 °C [4,5]. It is also known that REOs [12,13] as well as ZrO_2 [14–16] and CeO_2-ZrO_2 [17] have unique character to catalyze the dehydration of 2-alcohol to produce α-olefin via Hoffman elimination. We have also reported the dehydration of 1,4-butanediol as well as 1,5-pentanediol over composite oxides of cubic $Sc_{2-x}Yb_xO_3$ (x = 0.5, 1.0, and 1.5) [18]: the highest selectivity to 3-buten-1-ol surpassed 80% in the dehydration of 1,4-butanediol over the $Sc_{2-x}Yb_xO_3$ (x = 0.5, 1.0, and 1.5) catalysts calcined at 800 °C. Thus, we expected that REOs could work effectively in the dehydration of amino alcohols.

In this work, we investigated the dehydration of 5-amino-1-pentanol into 4-penten-1-amine over REOs and $Sc_{2-x}Yb_xO_3$ (x = 0.5, 1.0, and 1.5) at 425 °C to search a suitable catalyst and the efficient reaction conditions. We have found that 4-penten-1-amine is efficiently produced over Tm_2O_3, Yb_2O_3, and Lu_2O_3 in the dehydration of 5-amino-1-pentanol (Scheme 1). We also investigated the catalytic features of Yb_2O_3 in the dehydration of 5-amino-1-pentanol. Furthermore, we performed other amino alcohols with different carbon chain length, such as 3-amino-1-propanol, 4-amino-1-butanol, and 6-amino-1-hexanol, to produce the corresponding unsaturated amines over Yb_2O_3.

2. Experimental

2.1. Catalyst samples

Metal nitrate hydrates, such as $Ce(NO_3)_3$, $Nd(NO_3)_3$, $Sm(NO_3)_3$, $Eu(NO_3)_3$, $Gd(NO_3)_3$, $Tb(NO_3)_3$, $Ho(NO_3)_3$, $Y(NO_3)_3$, $Er(NO_3)_3$,

* Corresponding author.
E-mail address: satoshi@faculty.chiba-u.jp (S. Sato).

http://dx.doi.org/10.1016/j.apcata.2016.03.001
0926-860X/

Scheme 1. Dehydration of 5-amino-1-pentanol to 4-penten-1-amine.

$Tm(NO_3)_3$, $Yb(NO_3)_3$, $Lu(NO_3)_3$, and $Sc(NO_3)_3$, were purchased from Sigma-Aldrich Co., Ltd., Japan. La_2O_3, Pr_6O_{11}, $Mg(NO_3)_2$, $Ca(NO_3)_2$, and $Dy(NO_3)_3$ hexahydrate were purchased from Wako Pure Chemicals Co., Japan. 5-Amino-1-pentanol, 3-amino-1-propanol, and 4-amino-1-butanol were purchased from Wako Pure Chemicals Co., Japan. 6-Amino-1-hexanol aqueous solution (70 wt.%) was purchased from Sigma-Aldrich Co., Ltd., Japan.

Except La_2O_3 and Pr_6O_{11}, other REOs such as CeO_2, Nd_2O_3, Sm_2O_3, Eu_2O_3, Gd_2O_3, Tb_2O_3, Dy_2O_3, Ho_2O_3, Y_2O_3, Er_2O_3, Tm_2O_3, Yb_2O_3, Lu_2O_3, and Sc_2O_3 were prepared by the calcination of the corresponding nitrate. MgO and CaO were also prepared by the calcination of the corresponding nitrate. Monoclinic Yb_2O_3 was supplied by Kanto Kagaku Co., Ltd., Japan. Three $Sc_{2-x}Yb_xO_3$ ($x = 0.5$, 1.0, and 1.5) catalysts were supplied by Daiichi Kigenso Kagaku Kogyo Co., Ltd., Japan [18]. Rutile TiO_2 (JRC-TIO-3) and anatase TiO_2 (JRC-TIO-4) were supplied by Catalyst Reference of Japan. Amorphous SiO_2 (CARiACT Q10) was supplied by Fuji Silycia Chemical Ltd. Monoclinic ZrO_2 (RSC HP) and tetragonal ZrO_2 were supplied by Daiichi Kigenso Kagaku Kogyo Co., Ltd., Japan and Saint-Gobain, respectively. Al_2O_3 (N611N) and SiO_2-Al_2O_3 (N631L) were purchased from Nikki Chemical Co., Ltd., Japan.

2.2. Catalytic reaction

The dehydration of amino alcohols, such as 5-amino-1-pentanol, 3-amino-1-propanol, 4-amino-1-butanol, and 6-amino-1-hexanol, were carried out in a fixed-bed down flow reactor with an inside diameter of 20 mm under the atmospheric pressure of either N_2 or H_2 gas. In each test, 0.5 g of catalyst was loaded into the reactor. Amino alcohols were dehydrated at temperatures between 300 and 450 °C. Prior to the reaction, the catalyst was preheated in the flow reactor in a carrier gas at the same temperature as the reaction temperature for 1 h. After the pretreatment, an amino alcohol was fed through the top of the reactor at a liquid feed rate of 1.71 $cm^3\ h^{-1}$, which corresponds to 16 $mmol\ h^{-1}$ for 5-amino-1-pentanol and $W/F = 31\ g_{cat.}\ h\ mol^{-1}$ where W is catalyst weight and F is a reactant feed rate, together with a carrier gas flow of 20 $cm^3\ min^{-1}$. An effluent mixture collected every hour was analyzed by gas chromatography (GC-8A, Shimadzu, Japan) with a capillary column of TC-5 (30m, GL Science Inc., Japan) over a temperature range controlled from 70 to 280 °C at a heating rate of 10 °C min^{-1}. The major products in the dehydration were 4-penten-1-amine, piperidine, tetrahydropyridine, δ-valerolactam, and *n*-pentyl amine.

Since the catalytic activity is stable in the similar manner to the previous works reported in the dehydration of diols [3–11], the conversion of 5-amino-1-pentanol and the selectivity to each product were averaged in the 1–5 h to evaluate the catalytic activity. The formation rate of the corresponding unsaturated amines per unit surface area [$mmol\ h^{-1}\ m^{-2}$] was calculated by using the feed rate of the reactant multiplied by the conversion and the selectivity divided by the catalyst weight and specific surface area.

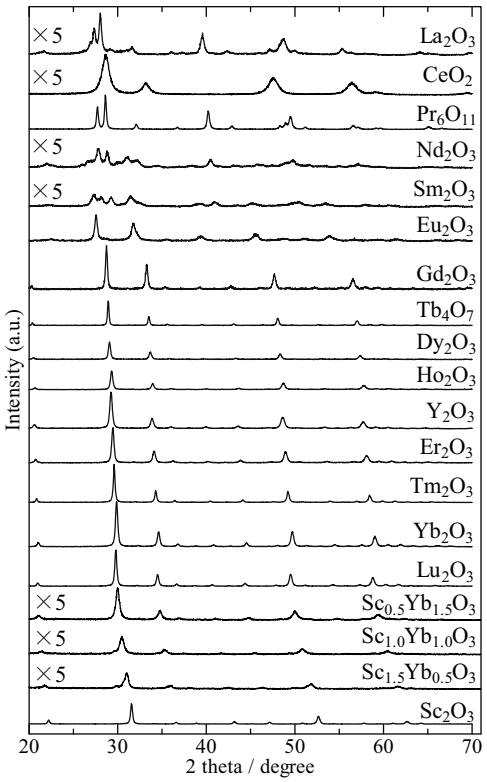

Fig. 1. XRD profiles of REO and $Sc_{2-x}Yb_xO_3$ samples calcined at 800 °C.

2.3. Characterization

The specific surface area (SA) of each catalyst was calculated by the BET method using the N_2 isotherm at −196 °C. X-ray diffraction (XRD) patterns were recorded on an XRD7000 (Shimadzu, Japan) using Cu Ka radiation (λ = 0.15 nm) to detect the crystal structure of the samples. The tube voltage and current were 40 kV and 40 mA, respectively.

Temperature-programmed desorption (TPD) of adsorbed CO_2 was measured to estimate the basicity of the catalysts. The numbers of basic sites were estimated from neutralization–titration curves of diluted NaOH solution [19,20]. Prior to the CO_2 adsorption, a sample (ca. 50 mg) was preheated in a quartz tube at 500 °C for 1 h under a reduced pressure. In CO_2-TPD, CO_2 was adsorbed on the sample at room temperature for 72 h and evacuated for 1 h. After no CO_2 had been observed in N_2 flow at room temperature, the sample was heated from room temperature to 800 °C at a heating rate of 10 °C min^{-1} in an N_2 flow of 34 $cm^3\ min^{-1}$. The desorbed CO_2 molecules, together with N_2 gas, were bubbled into an electric conductivity cell containing a dilute NaOH solution (50 cm^3). The conductivity of the solution was monitored, and the resulting conductivity curve was differentiated to provide a distribution curve of CO_2 desorbed from adsorbent.

3. Results

3.1. Characterization of REOs

Fig. 1 shows the XRD patterns of REOs and $Sc_{2-x}Yb_xO_3$ calcined at 800 °C. REO samples had different crystal structures with A-, B-, C-, and C_F-type [21,22]. Light REOs such as La_2O_3, Pr_6O_{11}, and Nd_2O_3 had a hexagonal structure of A-type. Other light REOs such as Sm_2O_3 had a monoclinic structure of B-type. On the other hand, heavy REOs such as Gd_2O_3, Tb_4O_7, Dy_2O_3, Ho_2O_3, Y_2O_3, Er_2O_3, Tm_2O_3, Yb_2O_3, Lu_2O_3, Sc_2O_3, and $Sc_{2-x}Yb_xO_3$ ($x = 0.5$, 1.0, and 1.5) [18] had a cubic bixbyite structure of C-type. Eu_2O_3 had an unknown phase, and CeO_2 had a cubic fluorite structure of C_F-type. The crystal phases of REOs and $Sc_{2-x}Yb_xO_3$ as well as their SA are summarized in Table 1.

Fig. 2 shows TPD profiles of CO_2 adsorbed on the REOs. Several desorption peaks of CO_2 from light REOs, such as La_2O_3, CeO_2,

Table 1
Dehydration of 5-amino-1-pentanol over REOs and $Sc_{2-x}Yb_xO_3$ catalysts at 425 °C[a].

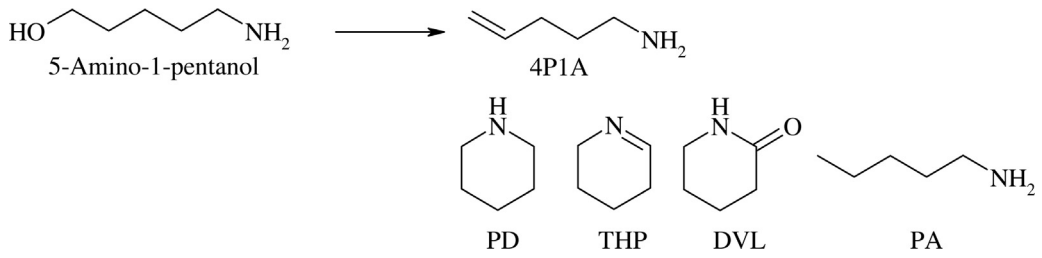

Catalyst	R_f[b]	SA	CP[c]	Conversion	Selectivity (mol%)[d]						Formation rate of
	(nm)	($m^2\ g^{-1}$)		(mol%)	4P1A	PD	THP	DVL	PA	Others	4P1A (mmol $h^{-1}\ m^{-2}$)
La_2O_3	0.1032	3.6	H	12.6	61.9	0	10.0	0	0	28.1	0.68
CeO_2	0.0970	92	C_F	70.1	56.8	1.6	3.9	5.5	18.2	14.0	0.14
Pr_6O_{11}	0.0990	55	H	13.4	66.0	19.3	0	0	0	14.7	0.05
Nd_2O_3	0.0983	11	H	17.5	81.3	2.2	7.9	0	0	8.7	0.40
Sm_2O_3	0.0958	5.7	M	17.1	43.7	11.7	0	0	0	44.6	0.41
Eu_2O_3	0.0947	13	Unknown	24.6	84.5	0	6.6	0	0	8.9	0.52
Gd_2O_3	0.0938	12	C	17.6	84.9	0	11.1	0	0	3.9	0.41
Tb_4O_7	0.0923	9.0	C	20.4	81.2	0	12.3	0	0	6.5	0.58
Dy_2O_3	0.0912	13	C	31.2	76.4	4.7	4.7	0	0	14.3	0.57
Ho_2O_3	0.0901	12	C	35.9	77.8	0	10.5	0	0	11.7	0.75
Y_2O_3	0.0900	19	C	58.0	81.6	0	4.8	0	3.1	10.5	0.79
Er_2O_3	0.0890	18	C	38.7	81.0	0	7.3	0	0	11.7	0.56
Tm_2O_3	0.0880	10	C	39.9	75.9	0	15.2	0	0	8.9	0.94
Yb_2O_3	0.0868	8.4	C	66.2	83.7	0	4.7	0	3.0	8.6	2.1
Lu_2O_3	0.0861	12	C	71.5	81.6	0	4.0	0	3.5	11.0	1.5
$Sc_{0.5}Yb_{1.5}O_3$	0.0837	26	C	56.7	83.3	0	8.8	0	2.5	5.5	0.60
$Sc_{1.0}Yb_{1.0}O_3$	0.0807	36	C	62.2	79.4	0	11.4	0	3.8	5.3	0.46
$Sc_{1.5}Yb_{0.5}O_3$	0.0776	53	C	70.5	74.5	9.2	8.8	0	2.6	4.9	0.34
Sc_2O_3	0.0745	29	C	89.0	21.4	74.0	0	0	0	4.6	0.21

[a] Conversion and selectivity were averaged in the 1–5 h. N_2 flow is 20 $cm^3\ min^{-1}$. $W/F = 31\ g_{cat.}\ h\ mol^{-1}$. Samples were calcined at 800 °C.
[b] Ionic radius of trivalent rare earth cation with coordination number 6, except Ce^{4+} with coordination number of 8 (Ref. [22]).
[c] CP, crystal phase: H, A-type hexagonal; M, B-type monoclinic; C, C-type cubic bixbyite; C_F, cubic fluorite.
[d] 4P1A, 4-penten-1-amine; PD, piperidine; THP, tetrahydropyridine; DVL, δ-valerolactam; PA, *n*-pentyl amine; Others, unidentified products.

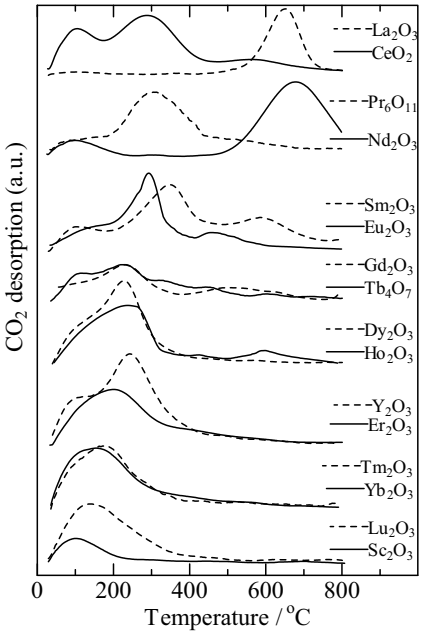

Fig. 2. TPD profiles of CO_2 adsorbed on REOs calcined at 800 °C.

Pr_6O_{11}, Nd_2O_3, Sm_2O_3, Eu_2O_3, Gd_2O_3, and Tb_4O_7, were observed at a wide temperature range between 100 and 800 °C. In contrast, over heavy REOs such as Dy_2O_3, Ho_2O_3, Y_2O_3, Er_2O_3, Tm_2O_3, Yb_2O_3, Lu_2O_3, and Sc_2O_3, desorption peaks were observed at low temperatures between 100 and 300 °C. The light REOs have strong basic sites, whereas heavy REOs have weak basic sites. These results are basically consistent with those of the previous report [22]. The desorption peak at the highest temperature in each REO had a tendency that the peak shifted to low temperatures as the atomic number decreases. However, TPD of adsorbed NH_3 was not performed because no adsorption of basic NH_3 on REOs was observed even at 25 °C [22].

3.2. Dehydration of 5-amino-1-pentanol over several acidic and basic catalysts

Table 2 lists catalytic activities of several oxide catalysts in the dehydration of 5-amino-1-pentanol. The conversion of 5-amino-1-pentanol and the selectivity to each product were averaged in the initial 1–5 h to evaluate the catalytic activity. Over Al_2O_3, SiO_2, SiO_2-Al_2O_3, TiO_2, and tetragonal ZrO_2, piperidine was dominantly produced. We have reported that acids catalyze the formation of saturated cyclic ether such as tetrahydrofuran and tetrahydropyran from the corresponding diols such as 1,4-butanediol and 1,5-pentanediol, respectively [3,23]. It is reasonable that these catalysts promote the piperidine formation. Over monoclinic ZrO_2, on the other hand, a small amount of 4-penten-1-amine was produced. Because monoclinic ZrO_2 has more basic sites than tetragonal sites [24], the monoclinic phase of ZrO_2 could catalyze the dehydration of 5-amino-1-pentanol at a high temperature of 375 °C. In other words, basic sites would work as the catalyst for the formation of 4-penten-1-amine in the dehydration of 5-amino-1-pentanol. In contrast to the acidic catalysts, basic MgO and CaO were inactive

Table 2
Dehydration of 5-amino-1-pentanol over several catalysts[a].

Catalyst[b]	SA ($m^2\ g^{-1}$)	Reaction temperature (°C)	Conversion (mol%)	Selectivity (mol%)[c]		
				4P1A	PD	Others
TiO_2 (rutile)	40	300	56.7	0	93.1	6.9
TiO_2 (anatase)	23	300	56.8	0	91.1	8.9
SiO_2	320	325	23.8	0	99.1	0.9
Al_2O_3	170	325	66.4	2.0	85.9	12.1
SiO_2-Al_2O_3	440	300	59.0	0.4	85.4	14.2
m-ZrO_2	46	375	40.6	12.8	64.5	22.7
t-ZrO_2	91	300	56.8	0	92.0	8.0
MgO	7.1	425	0.7	0	0	100
CaO	6.6	425	0.5	0	0	100

[a] Conversion and selectivity were averaged in the 1–5 h. Flow rate of N_2 carrier gas was 20 $cm^3\ min^{-1}$. $W/F = 31\ g_{cat.}\ h\ mol^{-1}$, where W and F are catalyst weight and flow rate of reactant feed, respectively.
[b] m-ZrO_2 means monoclinic ZrO_2, and t-ZrO_2 means tetragonal ZrO_2.
[c] Notation of products is the same as those in Table 1.

for the dehydration. Thus, we investigated rare earth oxides with basic sites in the following research.

3.3. Dehydration of 5-amino-1-pentanol over various rare earth oxide catalysts

Table 1 lists catalytic activities of various REOs and $Sc_{2-x}Yb_xO_3$ catalysts in the dehydration of 5-amino-1-pentanol at 425 °C. In all of the REOs, La_2O_3, CeO_2, Pr_6O_{11}, Sm_2O_3, and Sc_2O_3 showed the selectivity to 4-penten-1-amine lower than 70%. In particular, the selectivity to 4-penten-1-amine over Sc_2O_3 was the lowest among the REOs. Exceptionally, Sc_2O_3 produced piperidine with high selectivity. Over CeO_2, several by-products such as δ-valerolactam and *n*-pentyl amine were produced, whereas the conversion of 5-amino-1-pentanol was high. On the other hand, the other REOs such as Nd_2O_3, Eu_2O_3, Gd_2O_3, Tb_4O_7, Dy_2O_3, Ho_2O_3, Y_2O_3, Er_2O_3, Tm_2O_3, Yb_2O_3, Lu_2O_3, and $Sc_{2-x}Yb_xO_3$ showed the selectivity to 4-penten-1-amine higher than 70%. In particular, over Nd_2O_3, Eu_2O_3, Gd_2O_3, Tb_4O_7, Y_2O_3, Er_2O_3, Yb_2O_3, Lu_2O_3, and $Sc_{0.5}Yb_{1.5}O_3$, the selectivity to 4-penten-1-amine exceeded 80%, whereas the conversion of 5-amino-1-pentanol was lower than 40% over Nd_2O_3, Eu_2O_3, Gd_2O_3, Tb_4O_7, Dy_2O_3, Ho_2O_3, Er_2O_3, and Tm_2O_3. Over Y_2O_3, Yb_2O_3, Lu_2O_3, and $Sc_{0.5}Yb_{1.5}O_3$, the conversion exceeded 50% with the selectivity higher than 80%. Especially, over Yb_2O_3 and Lu_2O_3 calcined at 800 °C, the formation rate of 4-penten-1-amine per unit surface area exceeded 1 $mmol\ h^{-1}\ m^{-2}$. The three $Sc_{2-x}Yb_xO_3$ (x = 0.5, 1.0, and 1.5) catalysts with lattice constants between Yb_2O_3 and Sc_2O_3 showed a tendency to decrease the selectivity to 4-penten-1-amine from 83.3 to 74.5% with decreasing Yb content.

3.4. Dehydration of 5-amino-1-pentanol over Yb_2O_3

We have found that Yb_2O_3 performed the best formation rate of 4-penten-1-amine in REO catalysts. Therefore, we investigated the dehydration of 5-amino-1-pentanol over Yb_2O_3 prepared under different conditions. Table 3 lists the dependency of calcination temperature of Yb_2O_3 on the catalytic activity in the dehydration of 5-amino-1-pentanol into 4-penten-1-amine at 425 °C. The conversion of 5-amino-1-pentanol and the selectivity to 4-penten-1-amine were maximized at a calcination temperature of 800 °C. At calcination temperatures of 900 °C or higher, the conversion decreased with increasing calcination temperature. This is due to decrease in specific surface area. On the other hand, the selectivity to 4-penten-1-amine maintains approximately 80% irrespective to the calcination temperature. In short, Yb_2O_3 calcined at 800 °C showed the highest values in the conversion and the selectivity to 4-penten-1-amine. We also performed the dehydration over monoclinic Yb_2O_3 calcined at 500 °C for 3 h. Monoclinic Yb_2O_3 showed a lower selectivity to 4-penten-1-amine than cubic bixbyite Yb_2O_3 because of the formation of THP.

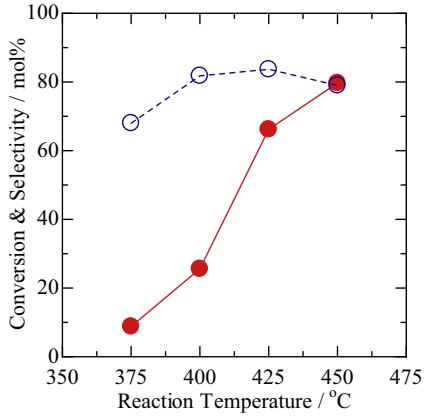

Fig. 3. Dependence of reaction temperature on (closed circle) 5-amino-1-pentanol conversion and (open circle) selectivity into 4-penten-1-amine over Yb_2O_3. Calcination temperature, 800 °C; *W/F*, 31 $g_{cat.}\ h\ mol^{-1}$.

Fig. 3 shows the conversion and the selectivity in the dehydration of 5-amino-1-pentanol into 4-penten-1-amine at different reaction temperatures over Yb_2O_3 calcined at 800 °C. The conversion monotonously increased from 9.4 to 80.8% with increasing reaction temperature. The selectivity to 4-penten-1-amine showed the highest level, 83.7%, at 425 °C. For the dehydration of 5-amino-1-pentanol, we calculated an apparent activation energy in an Arrhenius plot at temperatures between 375 and 425 °C to be 150 $kJ\ mol^{-1}$.

Fig. 4 presents the effect of contact time, W/F, on the conversion of 5-amino-1-pentanol and the selectivity to 4-penten-1-amine at 425 °C over Yb_2O_3 calcined at 800 °C. The conversion of 5-amino-1-pentanol increased with increasing W/F, whereas the selectivity to 4-penten-1-amine slightly decreased. At a large contact time, i.e. $W/F = 93\ g\ h\ mol^{-1}$ using 1.5 g of catalyst, the conversion of 5-amino-1-pentanol was 85.0% with the selectivity of 76.3%. This result indicates that the excessive reaction, such as the hydrogenation of 4-penten-1-amine into *n*-pentyl amine, rarely proceeds even at a high contact time, W/F.

3.5. Dehydration of 5-amino-1-pentanol over Yb_2O_3 in different carrier gases

Table 4 summarizes conversion and selectivity in the dehydration of 5-amino1-pentanol over Yb_2O_3 at 425 °C in different carrier gases. In H_2 flow instead of N_2, the conversion of 5-amino-1-pentanol decreased from 66.2 to 58.4%, while the selectivity to

Table 3
Dehydration of 5-amino-1-pentanol over Yb_2O_3 at different calcination temperatures.

Temperature (°C)	SA ($m^2\ g^{-1}$)	CP	Conversion (mol%)	Selectivity (mol%)				4P1A formation rate (mmol $h^{-1}\ m^{-2}$)
				4P1A	THP	PA	Others	
500	37	C	63.8	79.8	2.8	3.3	14.1	0.44
600	21	C	58.8	77.8	3.1	3.6	15.5	0.68
700	17	C	59.9	80.7	2.1	2.7	14.5	0.83
800	8.4	C	66.2	83.7	4.7	3.0	8.6	2.1
900	7.6	C	46.9	80.1	4.7	3.2	12.0	1.6
1000	6.9	C	39.1	80.9	3.7	2.4	12.9	1.4
500	47	M	73.3	74.5	6.1	3.9	15.5	0.36

Reaction conditions, symbols, and notation of products are the same as those in Table 1.

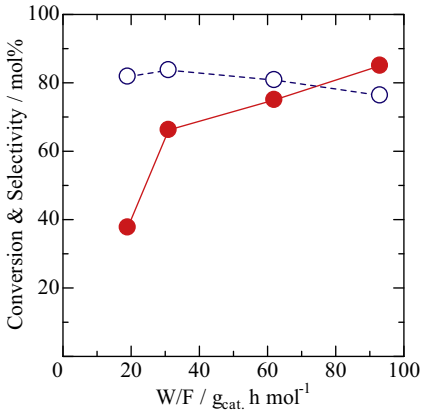

Fig. 4. Dependence of contact time on (closed circle) 5-amino-1-pentanol conversion and (open circle) selectivity to 4-penten-1-amine over Yb_2O_3 at 425 °C. Calcination temperature, 800 °C.

Table 4
Dehydration of 5-amino-1-pentanol over Yb_2O_3 in different carrier gases.

Carrier gas	Conversion (mol%)	Selectivity (mol%)[b]				
		4P1A	PD	THP	PA	Others
N_2	66.2	83.7	0	4.7	3.0	8.6
H_2	58.4	90.0	0	3.5	2.4	4.1
$N_2 + NH_3$[a]	45.7	85.3	0	3.0	2.7	9.0
CO_2	100	0	0	0	0	100 (unrecovered)
N_2[b]	47.6	14.4	78.4	0.2	0.0	7.0

Reaction conditions and notation of products are the same as those in Table 1. Total flow rate of carrier gas was 20 $cm^3\ min^{-1}$.
[a] N_2 (15 $cm^3\ min^{-1}$) + NH_3 (5 $cm^3\ min^{-1}$) was used.
[b] The sample was modified by impregnation with H_3PO_4 in Ref. [19].

4-penten-1-amine increased from 83.7 to 90.0%. It was found that the formation of by-products was suppressed in H_2 flow. In order to clarify the role of acidic and basic sites of Yb_2O_3, NH_3 and CO_2 were used as a poisoning gas in the following.

Although no adsorption of basic NH_3 to REOs is observed even at 25 °C [7], in basic NH_3 flow, the conversion of 5-amino-1-pentanol decreased without significant change in the selectivity to 4-penten-1-amine: the formation rate of 4-penten-1-amine was approximately three fourths of the rate in N_2 flow over Yb_2O_3 calcined at 800 °C. This means that basic NH_3 gas also affects the active sites of Yb_2O_3. On the other hand, CO_2 carrier gas was used in order to poison basic sites, but no dehydration products were observed: in acidic CO_2 flow, two equivalents of 5-amino-1-pentanol reacted with carbon dioxides and ammonium salt were formed in the vapor phase.

We attempted to impregnate Yb_2O_3 calcined at 800 °C with H_3PO_4 aqueous solution to poison the basic sites. H_3PO_4 was impregnated onto the sample to neutralize 70% of basic sites determined in CO_2-TPD. After, the sample was dried overnight at 110 °C and used. The conversion and the selectivity to 4-penten-1-amine decreased, on the other hand, piperidine was produced and the selectivity to piperidine reached to ca. 80%. These issues should be taken into consideration when we discuss the reaction mechanism.

Table 5
Dehydration of amino alcohols over Yb_2O_3[a].

Reactant	Reaction temperature (°C)	Conversion (mol%)	Selectivity (mol%)	
			Unsaturated amine	Others[a]
3-amino−1-propanol[b]	375	12.3	26.7	73.3
	400	48.0	36.9	63.1
	425	70.7	36.1	63.9
4-amino−1-butanol[c]	400	13.8	35.2	64.8
	425	53.3	44.5	55.5
6-amino−1-hexanol[d]	425	9.5	70.0	30.0
	450	66.4	88.1	11.9[d]

[a] Conversion and selectivity were averaged in the 1–5 h. H_2 flow is 20 $cm^3\ min^{-1}$. The sample was calcined at 800 °C. Others: unknown and unrecoverd products.
[b] Unsaturated amine is allylamine. $W/F = 22\ g_{cat.}\ h\ mol^{-1}$.
[c] Unsaturated amine is 3-buten-1-amine. $W/F = 25\ g_{cat.}\ h\ mol^{-1}$.
[d] Unsaturated amine is 5-hexen-1-amine. 70 wt.% 6-amino-1-hexanol aqueous solution was used. $W/F = 49\ g_{cat.}\ h\ mol^{-1}$. ε-Caprolactam was detected as a by-product with the selectivity of 4.8 mol%.

3.6. Dehydration of several amino alcohols over Yb_2O_3

The reactivity of 5-amino-1-pentanol with other amino alcohols, such as 3-amino-1-propanol, 4-amino-1-butanol, and 6-amino-1-hexanol over Yb_2O_3 calcined at 800 °C are compared in Table 5. The conversions of 3-amino-1-propanol and 4-amino-1-butanol increased with increasing reaction temperature. However, the selectivities to allylamine and 3-buten-1-amine were lower than that of 4-penten-1-amine because many by-products were produced in the dehydration of 3-amino-1-propanol and 4-amino-1-butanol. Consequently, in the dehydration of amino alcohols with short carbon chains of C3 and C4, it is concluded that Yb_2O_3 is ineffective.

In the dehydration of 6-amino-1-hexanol, in contrast, the conversion dramatically increased from 9.5 to 66.4% with increasing reaction temperature. Additionally the selectivity increased up to ca. 90% at 450 °C.

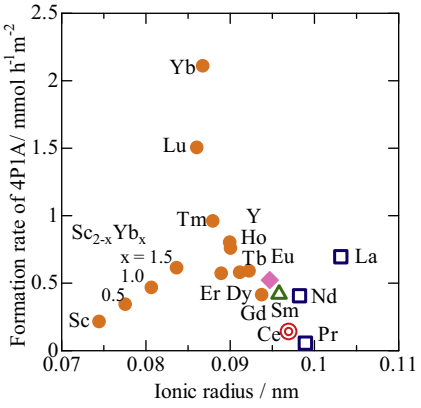

Fig. 5. Changes in the formation rate of 4-penten-1-amine at 425 °C with different ionic radius of rare earth cations of REO catalysts. Calcination temperature, 800 °C. Crystal phases: (open square) A-type hexagonal, (open triangle) B-type monoclinic, (closed circle) C-type cubic bixbyite, (double circle) cubic fluorite, and (closed diamond) unknown phase.

4. Discussion

4.1. Dehydration of 5-amino-1-pentanol over various rare earth oxides

In our previous work, we have reported that the dehydration of alkanediol is affected by crystal structures [5–9]. In a similar manner as the dehydration of alkanediol, we suppose that crystal structures contribute to the dehydration of 5-amino-1-pentanol. In Table 1, it is clear that REOs with the C-type bixbyite structure efficiently catalyze the dehydration of 5-amino-1-pentanol to produce 4-penten-1-amine. Among the cubic bixbyite REOs, Sc_2O_3 is the exception: piperidine is mainly formed over Sc_2O_3. It is speculated that either the weakest basicity or the smallest distance between the surface cations of Sc_2O_3 among the REOs [22] could be the cause of the distinctive behavior of Sc_2O_3. In the dehydration of 1,5-pentanediol, however, Sc_2O_3 produces mainly 4-penten-1-ol with a minor product of tetrahydropyran [4].

We have investigated the amount of basic sites of REOs in the previous section (Fig. 2). No acidic sites are observed in the adsorption of NH_3 on REOs even at 25 °C [22]. In the CO_2-TPD on the REOs, CO_2 desorption peaks that depend on the strength of the basic sites are observed. Light REOs, such as La_2O_3, Pr_6O_{11}, Nd_2O_3, and Sm_2O_3, have strong basic sites. In contrast, heavy REOs, such as Dy_2O_3, Ho_2O_3, Y_2O_3, Er_2O_3, Tm_2O_3, Yb_2O_3, Lu_2O_3, and Sc_2O_3, have weak basic sites. It is probable that the dehydration of 5-amino-1-pentanol is influenced by weak basic sites. Actually, Nd_2O_3 owes strong basic sites as well as weak basic sites at around 100 °C and showed high selectivity to 4-penten-1-amine (Table 1). As a pioneering work, it has been reported that the strength of the basic sites of La_2O_3, Sm_2O_3, Eu_2O_3, and Yb_2O_3 measured with thermal desorption of CO_2 decreases with increasing the atomic number of lanthanide metals [22,25]. The strength of the basic sites of REOs could be correlated with lanthanide contraction which decreases with decreasing radius of the rare earth cation.

Fig. 5 summarizes the intrinsic catalytic activity of REOs and $Sc_{2-x}Yb_xO_3$ catalysts with ionic radius of rare earth cation. The formation rate of 4-penten-1-amine per unit surface area increased with decreasing ionic radius of rare earth cation from La to Yb and decreased from Yb to Sc: the formation rate over Yb_2O_3 was the largest among those over the REOs and $Sc_{2-x}Yb_xO_3$ catalysts. These results indicate that the dehydration of 5-amino-1-pentanol is affected by the crystal structure, the strength of basic sites, and ionic radius of rare earth cations. These factors of the dehydration of 5-amino-1-pentanol are similar to those of the dehydration of 1,5-pentanediol [4], 1,4-butanediol [7], and 1,3-butanediol [9]. In the dehydration of 1,5-pentanediol and 1,4-butanediol, cubic Yb_2O_3 is active and selective (the formation rate of 4-penten-1-ol over Yb_2O_3 = 0.75 mmol h^{-1} m^{-2} at 400 °C in Table 2 of Ref. [18] and the formation rate of 3-buten-1-ol over Yb_2O_3 = 1.6 mmol h^{-1} m^{-2} at 350 °C in Table 3 of Ref. [18]). However, in the dehydration of 1,3-butanediol, fluorite CeO_2 is exceptionally active [5,8].

It is known that the radius of rare earth cation is correlated with the lattice parameter of the REO crystal structure. In other words, a distance between the adsorption sites depending on the lattice parameter could influence the catalytic nature of REOs. We have previously reported that REOs with hexagonal and monoclinic structures show lower activity than those with a cubic bixbyite structure. For example, the distance between La^{3+} cations in a hexagonal La_2O_3 [26] is calculated to be 0.394 nm, which is longer than those between other rare earth cations: Lu^{3+}, 0.367 nm; Yb^{3+}, 0.369 nm; Tm^{3+}, 0.371 nm in the cubic structure. The distance between rare earth cations is too long to dehydrate efficiently over REOs with the hexagonal structure. As another example of monoclinic Sm_2O_3 [27], a distance between Sm^{3+} cations is 0.363 nm, which is as long as that of Lu^{3+} cations in cubic bixbyite Lu_2O_3 with high activity. Thus, the catalytic activity of REOs with the monoclinic structure could be affected by other factors rather than only the distance between cations. We speculate that the main factor is the distance between the metal cation and the oxygen anion. However, we cannot conclude why catalytic activity of REOs with monoclinic structure was lower than that of REOs with the cubic bixbyite structure because the surface structure of REOs with monoclinic structure is insufficiently analyzed.

4.2. Proposed mechanism of 5-amino-1-pentanol dehydration

In the Section 3.4, we performed the dehydration of 5-amino-1-pentanol over Yb_2O_3 with different calcination temperatures. Over Yb_2O_3 with cubic bixbyite phase in Table 3 (XRD figure not shown), the formation rate per unit surface area is maximized at 800 °C. In contrast to the cubic bixbyite structure, over monoclinic Yb_2O_3 calcined at 500 °C for 3 h, both the selectivity to 4-penten-1-amine and the formation rate per unit surface area are lower than those over cubic Yb_2O_3. These results indicate that cubic bixbyite Yb_2O_3 provides suitable surface in the dehydration of 5-amino-1-pentanol. In the dehydration of 5-amino-1-pentanol, the reaction would probably proceed over the oxygen defect sites {2 2 2} facet of bixbyite Yb_2O_3 in a similar way to the dehydration of 1,5-pentanediol [4] and 1,4-butanediol [7].

We have reported a model structure of the active center in the dehydration of 1,4-butanediol (Fig. 7 of Ref. [7]). We have also calculated the adsorption energy of 1,4-butanediol on {2 2 2} facet of bixbyite REO surface [28]. In the similar manner as the dehydration of 1,4-butanediol, we depicts an adsorption model of 5-amino-1-pentanol on acid-base center (Fig. 6). The active center is composed of one basic site and two acidic sites. The basic site is an oxygen anion, and the acidic sites are Yb^{3+} cations. They are located on the {2 2 2} facet of bixbyite crystal [29]. In Fig. 6, we speculate the dehydration mechanism of 5-amino-1-pentanol in the following route. Firstly, the OH and NH_2 group of the reactant adsorb on either of acidic sites, and a hydrogen atom of position 2 of CH_2 group is activated by the basic site to form tridentate coordination. Secondly, the hydrogen atom is abstracted by the basic site as a form of proton, and then the OH group is abstracted by the acidic site, which completes the formation of C=C bond. Finally, the NH_2 group is desorbed, whereby 4-penten-1-amine and H_2O are generated.

In Table 4, we have performed the poisoning experiment of Yb_2O_3 that the formation rate of 4-penten-1-amine is markedly suppressed over Yb_2O_3 poisoned by H_3PO_4. This signifies that the basic sites poisoned by H_3PO_4 play an important role in the acti-

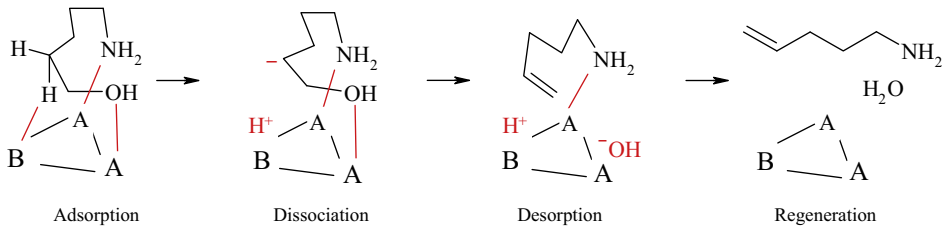

Fig. 6. Probable reaction mechanism of the dehydration of 5-amino-1-pentanol to produce 4-penten-1-amine over Yb_2O_3. A and B in the figure indicate acidic and basic sites, respectively.

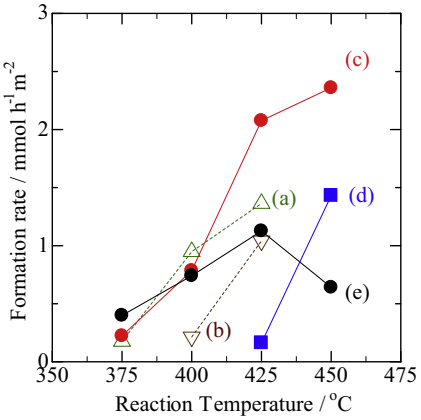

Fig. 7. Changes in the dehydration ability of Yb_2O_3 calcined at 800 °C in the dehydration of amino alcohols into corresponding unsaturated amines with reaction temperature. (a) 3-amino-1-propanol, the formation rate of allylamine; (b) 4-amino-1-butanol, the formation rate of 3-buten-1-amine; (c) 5-amino-1-pentanol, the formation rate of 4-penten-1-amine; (d) 6-amino-1-hexanol, the formation rate of 5-hexen-1-amine over Yb_2O_3 in this work; and (e) 1,5-pentanediol over Yb_2O_3, the formation rate of 4-penten-1-ol which is calculated from the data of Yb_2O_3 calcined at 800 °C in Ref. [4].

vation of 5-amino-1-pentanol to produce 4-penten-1-amine. On the other hand, in NH_3 flow, the formation rate is also suppressed. Although NH_3 is not adsorbed on REOs at 25 °C [7], we speculate that abundant NH_3 could be able to block the adsorption sites of Yb_2O_3 at 425 °C, and that NH_3 would adsorb on the acidic sites competing with the amino group of the reactant. It is reasonable that very weak acidic sites of Yb_2O_3 work as anchoring sites of the amino group, and that they cooperate with basic sites to form active sites. Thus, both basic and acidic sites would participate in the formation of 4-penten-1-amine via an acid-base concerted tridentate coordination mechanism (Fig. 6).

4.3. Reactivity of amino alcohols into unsaturated amines over Yb_2O_3

In the dehydration of 5-amino-1-pentanol, 3-amino-1-propanol, 4-amino-1-butanol, and 6-amino-1-hexanol, Yb_2O_3 catalyzes the formation of unsaturated amines. As shown in Table 5, the conversion of amino alcohols generally increased with increasing reaction temperature. In order to compare the reactivity of amino alcohols, Fig. 7 illustrates the formation rate of the corresponding unsaturated amines over Yb_2O_3 calcined at 800 °C as a function of reaction temperature. The formation rate of unsaturated amines in these reactions clearly indicates the difference in the reactivity of these amino alcohols. At 425 °C, it is found that the reactivity of amino alcohols over Yb_2O_3 is the following order: 5-amino-1-pentanol > 3-amino-1-propanol > 4-amino-1-butanol ≫ 6-amino-1-hexanol. Although 3-amino-1-propanol is reactive in the dehydration over Yb_2O_3, the selectivity to allylamine is quite low at 375–425 °C (Table 5). Similarly, 4-amino-1-butanol is actively converted over Yb_2O_3 at 425 °C but the selectivity is low. On the contrary, the dehydration of 6-amino-1-hexanol is much less reactive than the other amino alcohols at 425 °C. However, it is attractive that the dehydration of 6-amino-1-hexanol is selective since the selectivity to 5-hexen-1-amine is 88.1% at 450 °C.

We have previously investigated the dehydration of 1,5-pentanediol over Yb_2O_3 [4]: Yb_2O_3 calcined at 800 °C is preferable in the reaction. In Fig. 7, the formation rate of 4-penten-1-ol at 425 °C, which was calculated from the data presented in Fig. 7 of Ref. [4], was plotted as a reference to those of amino alcohols. Although 1,5-pentanediol has the same number of carbon atoms in the chain as 5-amino-1-pentanol, the formation rate of 4-penten-1-ol at 425 °C is at most 1.1 mmol h^{-1} m^{-2} and the value is about a half of that of 5-amino-1-pentanol. The difference in the reactivity between 5-amino-1-pentanol and 1,5-pentanediol could be explained by the difference in the adsorption strength between 5-amino-1-pentanol and 1,5-pentanediol: the amino group is more strongly anchored onto the surface than the hydroxyl group.

In the previous section, we discussed the reaction mechanism from adsorption to regeneration that one molecule of 5-amino-1-pentanol adsorbed on three sites of the catalyst surface, where two acidic sites and one basic site of bixbyite REO surface. As results of computational molecular modeling, over the active center with triangle shape, 6-amino-1-hexanol always forms a cis-conformation in the dihedral angle of four methylene chains. In contrast, the other reactive amino alcohols such as 4-amino-1-butanol and 5-amino-1-pentanol can form only gauche-conformation in the adsorption model. The adsorption structure could be strained by the cis-conformation. This could be the cause of the low reactivity of 6-amino-1-hexanol. Thus, we speculate the adsorption structure of amino alcohols but there still remain questions. We will continue to further study to confirm the above-mentioned speculation.

5. Conclusions

Vapor-phase dehydration of 5-amino-1-pentanol was investigated over REO_s and $Sc_{2-x}Yb_xO_3$ (x = 0.5, 1.0, and 1.5) at 425 °C. In the conversion of 5-amino-1-pentanol over REOs calcined at 800 °C, 4-penten-1-amine was produced rather than the formation of a cyclic amine, piperidine. Yb_2O_3, Lu_2O_3, and Tm_2O_3 with the cubic bixbyite structure showed selectivity to 4-penten-1-amine higher than 80%, while REOs with hexagonal and monoclinic structures showed low selectivity. Especially, Yb_2O_3 calcined at 800 °C showed high formation rate of 4-penten-1-amine over 2 mmol h^{-1} m^{-2} at 425 °C. Over Yb_2O_3 catalyst, the conversion of 5-amino-1-pentanol was reached up to 85.0% with the selectivity to 4-penten-1-amine around 76% at 425 °C and W/F of 93 $g_{cat.}$ h mol^{-1}.

The reactivity of amino alcohols into the corresponding unsaturated amines over Yb_2O_3 calcined at 800 °C was the order of 5-amino-1-pentanol > 3-amino-1-propanol > 4-amino-1-butanol > 6-amino-1-hexanol. The results suggest that the dehydration of the amino alcohols is affected by the carbon chain length

of amino alcohols, the crystal structure of REOs, and ionic radius of rare earth cations.

References

[1] B. Zimmermann, J. Herwig, M. Beller, Angew. Chem. Int. Ed. 38 (1999) 2372–2375.
[2] S. Nicolai, R. Sedigh-Zadeh, J. Waser, J. Org. Chem. 78 (2013) 3783–3801.
[3] S. Sato, R. Takahashi, N. Yamamoto, E. Kaneko, H. Inoue, Appl. Catal. A: Gen. 334 (2008) 84–91.
[4] F. Sato, H. Okazaki, S. Sato, Appl. Catal. A: Gen. 419–420 (2012) 41–48.
[5] S. Sato, F. Sato, H. Gotoh, Y. Yamada, ACS Catal. 3 (2013) 721–734.
[6] F. Sato, Y. Yamada, S. Sato, Chem. Lett. 41 (2012) 593–594.
[7] S. Sato, R. Takahashi, M. Kobune, H. Inoue, Y. Izawa, H. Ohno, K. Takahashi, Appl. Catal. A: Gen. 356 (2009) 64–71.
[8] M. Kobune, S. Sato, R. Takahashi, J. Mol. Catal. A: Chem. 279 (2008) 10–19.
[9] S. Sato, R. Takahashi, T. Sodesawa, A. Igarashi, H. Inoue, Appl. Catal. A: Gen. 328 (2007) 109–116.
[10] T. Nozawa, S. Sato, R. Takahashi, Top. Catal. 52 (2009) 609–617.
[11] H. Gotoh, Y. Yamada, S. Sato, Appl. Catal. A: Gen. 377 (2010) 92–98.
[12] A.J. Lundeen, R.V. Hoozer, J. Org. Chem. 32 (1967) 3386–3389.
[13] S. Bernal, J.M. Trillo, J. Catal. 66 (1980) 184–190.
[14] B.H. Davis, P. Ganesan, Ind. Eng. Chem. Prod. Res. Dev. 18 (1979) 191–198.
[15] S. Chokkaram, B.H. Davis, J. Mol. Catal. A: Chem. 118 (1997) 89–99.
[16] M.A. Aramendía, V. Borráu, C. Jiménez, J.M. Marinas, A. Marinas, A. Porras, F.J. Urbano, J. Catal. 183 (1999) 240–250.
[17] V. Solinas, E. Rombi, I. Ferino, M.G. Cutrufello, G. Colon, J.A. Navio, J. Mol. Catal. A: Chem. 204–205 (2003) 629–635.
[18] F. Sato, S. Sato, Catal. Commun. 27 (2012) 129–133.
[19] N. Yamamoto, S. Sato, R. Takahashi, K. Inui, J. Mol. Catal. A: Chem. 243 (2006) 52–59.
[20] S. Sato, K. Koizumi, F. Nozaki, J. Catal. 178 (1998) 264–274.
[21] G. Adachi, N. Imanaka, Chem. Rev. 98 (1998) 1479–1514.
[22] S. Sato, R. Takahashi, M. Kobune, H. Gotoh, Appl. Catal. A: Gen. 356 (2009) 57–63.
[23] H. Inoue, S. Sato, R. Takahashi, Y. Izawa, H. Ohno, K. Takahashi, Appl. Catal. A: Gen. 352 (2009) 66–73.
[24] S. Sato, J. Igarashi, Y. Yamada, Appl. Catal. A: Gen. 453 (2013) 213–218.
[25] V.R. Choudhary, V.H. Rane, J. Catal. 130 (1991) 411–422.
[26] P. Aldebert, J.P. Traverse, Mater. Res. Bull. 14 (1979) 303–323.
[27] T. Schleid, G. Meyer, J. Less Common Met. 149 (1989) 73–80.
[28] F. Sato, S. Sato, Y. Yamada, M. Nakamura, A. Shiga, Catal. Today 226 (2014) 124–133.
[29] M. Segawa, S. Sato, M. Kobune, T. Sodesawa, T. Kojima, S. Nishiyama, N. Ishizawa, J. Mol. Catal. A: Chem. 310 (2009) 166–173.